W. W. Schultz[1]
Mem. ASME

S. H. Davis

Department of Engineering Science
and Applied Mathematics,
The Technological Institute,
Northwestern University,
Evanston, Ill. 60201

Effects of Boundary Conditions on the Stability of Slender Viscous Fibers

The one-dimensional isothermal flow of viscous-liquid fibers displays draw resonance instability when a constant-velocity winder condition is applied. This instability is removed when a constant-force condition occurs at the winder. The instability mechanism is examined and used to explain the stability trends when the effects of gravity, surface tension, inertia, and wind stress are included.

Introduction

For sufficiently large winder speeds, man-made textile processes are susceptible to a "draw resonance" instability. This instability causes time-periodic variations in the fiber diameter which lowers product performance and can disrupt the spinning process by causing fiber breakage.

Textile process instabilities are commonly studied by examining a simple fiber system composed of a constant-property Newtonian liquid entering a passive gaseous environment. Heat transfer and complex rheology have major qualitative influences, although the basic stability mechanism remains the same as the simplified system. Furthermore, the axisymmetric flow is usually replaced by a one-dimensional flow in which the axial velocity depends only on time t and the axial coordinate z. Such a model is expected to describe the steady basic flow and its stability as long as the axial velocity for both vary slowly along the fiber axis and (axisymmetric) end effects are confined to short regions near the orifice and winder. Consequently, the one-dimensional stability model we use well represents only disturbance wavelengths long compared to the fiber radius. This means that capillary instabilities, with wavelengths on the order of the fiber radius, will be suppressed. This is not a serious limitation for most textile processes.

In this work we will discuss the one-dimensional theory containing modified orifice and winder boundary conditions and their effects on fiber stability characteristics for a viscous-dominated fiber. These results give insight into the mechanism of draw resonance which is useful in predicting trends in more complicated systems.

Formulation of the Stability Problem

A liquid jet (fiber) emerges at an average axial velocity w_i from an orifice of radius r_i into a passive gaseous environment. At a distance L, the fiber is "wound up" at a given average axial velocity w_w. Gravity acts in the z direction. The fluid density ρ and viscosity μ are constant as well as the surface tension γ on the liquid-gas interface. Figure 1 shows a schematic of the fiber system.

The unsteady system of viscous-dominated fibers was first given in [1] and the full system is given in [2]. The steady system is derived systematically from the axisymmetric equations of motion in [3]. In nondimensional form the one-dimensional continuity and axial momentum equations are:

$$(WA)_z + A_t = 0 \tag{1a}$$

$$Re(W_t + WW_z) - G - 3W_{zz} - 3A^{-1}A_z W_z - (2Ca)^{-1}A_z A^{-3/2} = 0. \tag{1b}$$

The boundary conditions for the unsteady problem are

$$W(0,t) = 1, \quad W(1,t) = \mathrm{E} = e^{\alpha}, \quad A(0,t) = 1, \tag{1c,d,e}$$

where subscripts z and t denote partial differentiation. Here, the cross-sectional fiber area A and axial velocity W have been scaled by their values at the orifice, viz., πr_i^2 and w_i, respectively. The axial distance z and time t have been scaled on L and L/w_i, where L is the distance between the orifice and winder. The dimensionless groups are

$$Re = w_i L\rho/\mu \tag{1f}$$

$$G = \rho L^2/\mu w_i \tag{1g}$$

$$Ca = w_i \mu r_i/\gamma L \tag{1h}$$

$$\alpha = ln\ E = ln(w_w/w_i). \tag{1i}$$

The steady solution to system (1) is the basic state $A = A_s(z)$, $W = W_s(z)$ which, in general, must be obtained numerically [2].

We examine the stability of the basic state by superposing small disturbances, linearizing, and using normal modes in time. These disturbed variables have the form

$$W(z,t) = W_s(z)[1 + w(z)e^{\sigma t}] \tag{2a}$$

$$A(z,t) = A_s(z)[1 + a(z)e^{\sigma t}]. \tag{2b}$$

[1] Present Address: Department of Mechanical and Aerospace Engineering, College of Engineering, Rutgers University, Piscataway, N.J. 08854.

Contributed by the Applied Mechanics Division for publication in the JOURNAL OF APPLIED MECHANICS.

Discussion on this paper should be addressed to the Editorial Department, ASME, United Engineering Center, 345 East 47th Street, New York, N.Y. 10017, and will be accepted until two months after final publication of the paper itself in the JOURNAL OF APPLIED MECHANICS. Manuscript received by ASME Applied Mechanics Division, May, 1983.

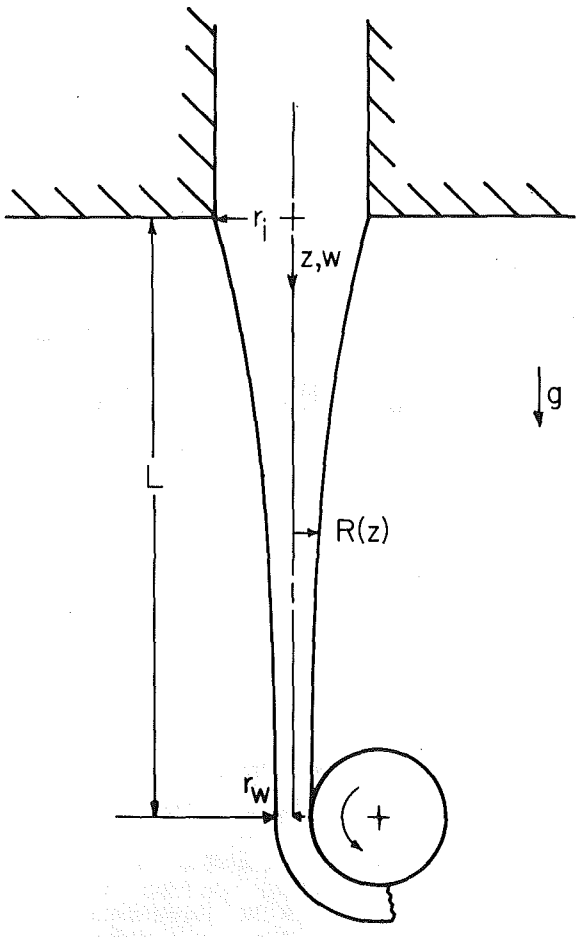

Fig. 1 Fiber coordinate system

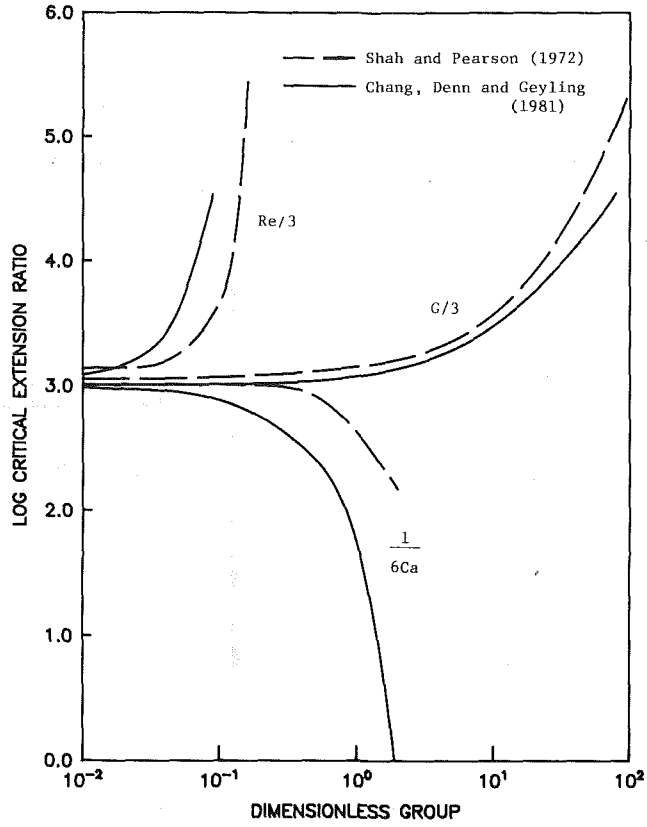

Fig. 2 Effect of gravity, surface tension, and inertia or fiber stability

where σ is the complex growth rate (eigenvalue) and a and w are complex-valued eigenfunctions. When $E=E_c$, the critical extension ratio, the real part of the growth rate is zero and the eigenvalue $\sigma=i\omega_c$, where ω_c is the frequency of oscillation at critical conditions. Factoring out the forms W_s and A_s (in effect scaling the disturbance quantities on the local basic-state values) simplifies the disturbance equations as compared to those obtained using $W=W_s+w$ and $A=A_s+a$.

The linearized disturbance equations become

$$a_z+w_z+A_s\sigma a=0 \tag{3a}$$

$$w_{zz}+(W_{s_z}A_sa_z)_z+A_sW_{s_z}a_z-Re[(\sigma+2W_{s_z})w + W_sw_z]/3+(6Ca)^{-1}W_s^{1/2}(A_sa_z-A_{s_z}a/2)=0. \tag{3b}$$

The disturbance boundary conditions from (1c–e) are

$$a(0)=0,\quad w(0)=0,\quad w(1)=0. \tag{3c,d,e}$$

The norm of the solution is set by

$$w_z(0)=1. \tag{3f}$$

The complex system (3) is broken into a set of six, first-order, real ordinary differential equations and integrated by a Gill-modified, Runge-Kutta shooting method.

The effect of individually varying gravity, surface tension, and inertia on α_c is shown in Fig. 2. The results of Fig. 2 are essentially those of Chang, Denn, and Geyling [4] who obtained more accurate values than the earlier results of Shah and Pearson [5]. Our independently obtained results are within 1 percent of those of [4]. Figure 2 shows that gravity and inertia stabilize the fiber while surface tension destabilizes the fiber. We will explain these trends after examining the instability mechanism for viscous-dominated fibers.

Comparisons With Experiments

There are three sets of experiments on isothermal, Newtonian fibers [6–8]. These are in general agreement with the one-dimensional stability analysis as shown in [8] and summarized in Table 1. The experimental critical draw ratios are generally within 20 percent of the predicted values. Average draw ratios are about 15 percent less than the predictions while frequencies are roughly 30 percent less than that predicted. The trends of increasing gravity, surface tension, and inertia appear correct. Inexplicably, the data of [8] have a frequency one-sixth the predicted value.

There are some ambiguities in comparing experiments to the theory because the actual flow is two-dimensional near the fiber ends. Two-dimensional corrections for the steady jet radius in the region away from the ends (based on [3]) are less than one-half percent for the typical data of [7]. However, the two-dimensional regions at the fiber ends have an axial extent of approximately one diameter [9]. From the slenderness ratio ϵ (the orifice radius divided by jet length) shown in Table 2, we see that the boundary layer at the orifice is 2–14 percent of the fiber length. To bypass this region, Chang and Denn [8] move the origin of their coordinate system to the point of maximum die swell. Although radial variations of the axial velocity are small at this point, it is obvious that one-dimensional theory is still not valid there since dR/dz of the one-dimensional model cannot vanish in an accelerating jet. They also assume that the radius of the die swell region is fixed during unsteady flow. There is no reason to expect this.

There are also difficulties in evaluating the boundary condition at the winder. Chang and Denn [8] note that the peripheral winder speed is considerably higher than the average axial fiber velocity at the winder. This is indeed necessary if the winder is to apply a tension to an isothermal jet. Chang and Denn use the average jet velocity at the winder (calculated from fiber diameter measurements) in comparison

Table 1 Experimental stability comparisons

r_i (cm)	ρ (g/cm^3)	σ (d/cm)	μ (poise)	L (cm)	w_i (cm/s)	E_c	T (s)
			Chang and Denn (1979)				
0.178	1.4	60.0	220	4	3.43	26.0	2.3
			Donnelly and Weinberger (1975)				
0.140	1.0	22.4	1000	2	1.04	17.0	1.2
0.140	1.0	22.4	1000	2	0.72	17.3	1.8
0.140	1.0	22.4	1000	2	0.50	17.2	1.4
0.140	1.0	22.4	1000	4	0.50	17.2	3.4
			D'Andrea and Weinberger (1976)				
0.120	1.0	22.4	1000	7.8	0.98	26.0	
0.120	1.0	22.4	1000	9.6	0.98	37.1	
0.120	1.0	22.4	1000	10.9	0.98	46.2	
0.093	1.0	22.4	1000	7.3	0.75	26.9	
0.120	1.0	22.4	1000	8.5	0.68	43.0	
0.120	1.0	22.4	1000	12.4	0.98	52.0	
0.075	1.0	22.4	1000	6.4	0.39	17.8	
0.120	1.0	22.4	1000	5.8	0.22	31.9	
0.075	1.0	22.4	1000	12.9	0.80	46.9	

Table 2 Analytical stability comparisons

$G/3$	$Re/3$	$Ca^{-1}/6$	ϵ	E_c	ω_c	T
			Chang and Denn (1979)			
9.7	0.02900	0.300	0.045	32.20	18.63	0.40
			Donnelly and Weinberger (1975)			
1.25	0.00069	0.051	0.070	20.78	14.67	0.82
1.81	0.00048	0.198	0.070	20.90	14.94	1.17
2.60	0.00033	0.285	0.070	21.05	15.32	1.64
10.4	0.00066	0.213	0.035	26.70	19.36	2.60
			D'Andrea and Weinberger (1976)			
20.2	0.0026	0.246	0.015	35.18	23.66	
30.6	0.0031	0.303	0.013	42.07	27.40	
39.4	0.0036	0.345	0.011	47.60	30.18	
23.2	0.0018	0.390	0.013	32.66	24.35	
34.8	0.0019	0.390	0.014	40.95	28.54	
51.1	0.0041	0.392	0.010	54.60	33.53	
34.0	0.0008	0.810	0.011	27.50	27.03	
49.2	0.0004	0.808	0.020	34.30	31.86	
68.1	0.0034	0.805	0.006	44.57	36.98	

of analysis to experiments but they still use the fixed jet speed winder boundary condition. Weinberger and coworkers use the winder speed in their calculations. Since there is slip between the wheel and fiber, a mixed boundary condition is more appropriate for the one-dimensional theory. These boundary conditions are analyzed further in the next section for the viscous-dominated case.

Winder Boundary Conditions

When gravity, surface tension, and inertia are neglected, the normal-mode disturbance equations and boundary conditions can be simplified to the following:

$$a_z + w_z + \sigma e^{-\alpha z} a = 0 \tag{4a}$$

$$w_{zz} + \alpha(a_z + w_z) = 0 \tag{4b}$$

$$a(0) = w(0) = w(1) = 0. \tag{4c,d,e}$$

The velocity can be eliminated to give the equivalent system:

$$a_{zz} + \sigma e^{-\alpha z} a_z = 0 \tag{5a}$$

$$a(0) = 0 \tag{5b}$$

$$a_z(1) - a_z(0) + (\sigma e^{-\alpha} - \alpha) a(1) = 0. \tag{5c}$$

Equation (5a) can be integrated directly to give

$$a = C_1 E_1\left(-\frac{\sigma}{\alpha} e^{-\alpha z}\right) + C_2, \tag{6}$$

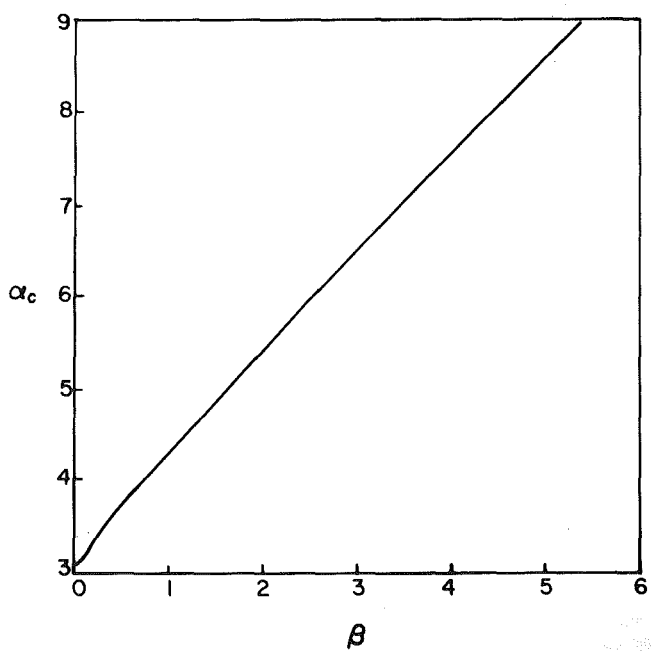

Fig. 3 Effect of winder slip on fiber stability

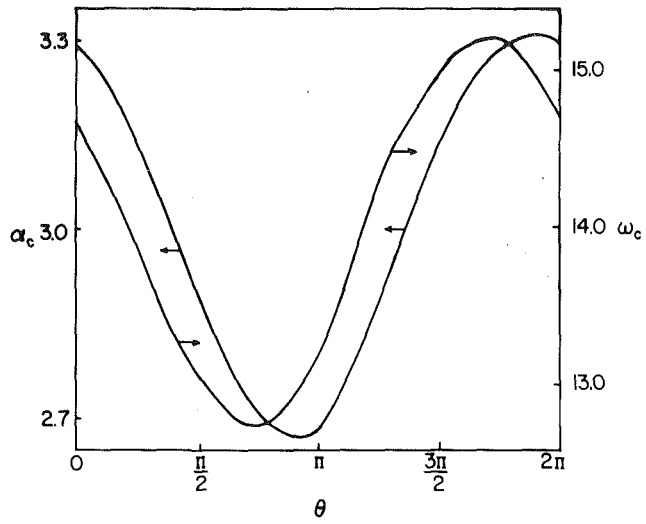

Fig. 4 Effect of winder boundary condition phase on critical α and ω

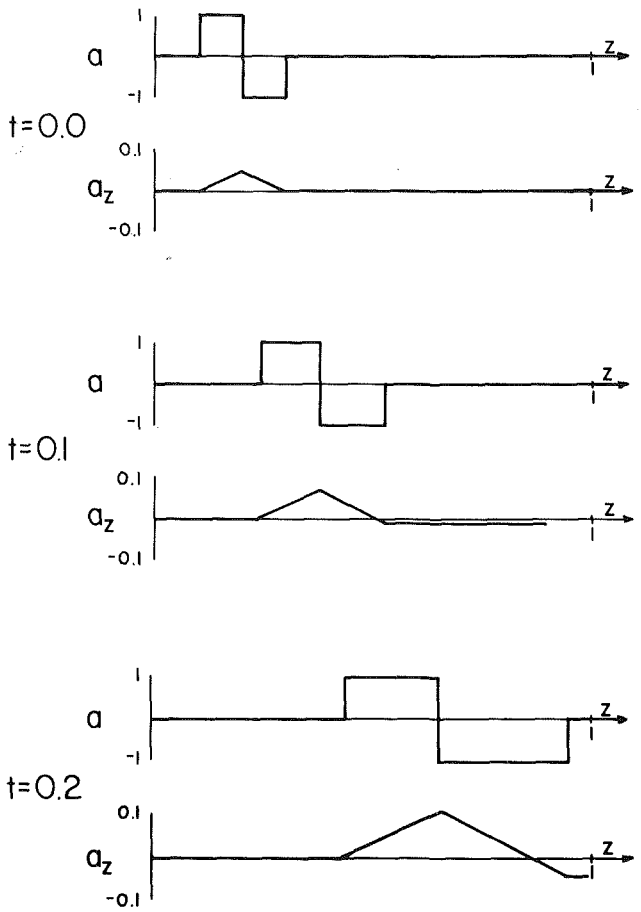

Fig. 5 Wave forms of disturbances for constant force winder

where E_1 is the exponential integral of the first kind and C_1 and C_2 are constants of integration. Application of boundary conditions gives the characteristic equation

$$e^{uv} - e^u + (uv-1)[E_1(-uv) - E_1(-u)] = 0, \tag{7}$$

where $u = \sigma/\alpha$ and $v = e^{-\alpha}$. This complex-valued equation can be solved by secant methods to find the now standard results [8, 10] very accurately:

$$\alpha_c = 3.006510\ (E_c = 20.21),\ \omega_c = 14.011.$$

As previously mentioned, a mixed (Robin) boundary condition would be more appropriate at the winder. This can be written as

$$w(1) + \beta f(1) = 0, \tag{8}$$

where f is the normal-mode amplitude of the force disturbance applied by the winder to the fiber. Now $\beta = 0$ represents the constant-velocity condition and $\beta = \infty$ represents the constant-force condition. Here, β might be a complex constant which could be determined experimentally. The value of β should depend on a number of factors but the real part should be positive since the fiber velocity at the winder should decrease as the resistance of the fiber to elongation increases. The force f is the integral of (4*b*),

$$f = w_z + \alpha(a + w). \tag{9}$$

If the orifice boundary condition remains as $a(0) = 0$, boundary condition (5*c*) is now replaced by

$$a_z(1) - (1+\beta)a_z(0) + (\sigma e^{-\alpha} - \alpha)a(1) = 0, \tag{10}$$

and the characteristic equation that replaces expression (7) is

$$e^{uv} - e^u + (uv-1)[E_1(-uv) - E_1(-u)] - \beta e^u = 0. \tag{11}$$

The critical α varies with β as shown in Fig. 3. The constant-velocity critical value is still $\alpha_c = 3.00657$ and the constant-force critical value approaches infinity so the jet appears to be *completely stabilized*. Kase and Denn [11] have mentioned without elaboration that the constant-force winder boundary condition stabilizes the fiber, and White and Ide [12] allude to this phenomenon. We note from (10) that as $\beta \to \infty$, the boundary value problem switches to an initial value problem. Thus, the eigenvalue character of the stability problem is lost.

Figure 3 indicates that fiber slippage at the winder increases the critical α and ω, which increases the disparity between predictions and experiments. If this disparity is due to slippage or the winder boundary condition in general, this could be caused by a phase difference between f and w. This phase would be a function of the winder motor characteristics, winder moment of inertia, etc. This phase lag θ is represented in equation (8) by a complex-valued β,

$$\beta = |\beta| e^{i\theta}. \tag{12}$$

As an example, Fig. 4 shows ω_c and α_c for $|\beta| = 0.2$ and $0 < \theta < 2\pi$. This shows that the predicted critical values can approach the experimental values when a phase θ is included in the model. Without further experimental information about the winder and an analysis near the orifice, we cannot proceed further.

The boundary conditions at the orifice could also be replaced by modified conditions at a new origin defined downstream of the point of maximum swell to avoid the two-dimensional region. With the added complexity of two boundary conditions at the orifice, this ad hoc approach seems unsatisfactory. Further study of unsteady flow near the orifice should examine the full axisymmetric equations.

The Instability Mechanism

The preceding analysis gives insight into the stability mechanism of draw resonance. When the winder boundary condition is that of constant force, the solution to the initial value problem can be solved by factoring the original disturbance equations (3) to show the hyperbolic character of the operator:

$$(\partial/\partial z + e^{-\alpha z}\partial/\partial t)\partial a/\partial z = 0, \tag{13a}$$

whose first integral is

$$a_z = G(t + e^{-\alpha z}/\alpha), \tag{13b}$$

where G is an arbitrary function. Equation (13*b*) can be further integrated to give the solution for a. These equations

first appeared in [2] and have been analyzed somewhat in [12]. The velocity of the wave of a_z from (13*a*) is seen to be the velocity of the basic state $e^{\alpha z}$, while the wave velocity of a is infinite. (This supports Denn's [13] criticism of the analysis by Hyun [14] who compared "wave residence time" with fluid residence time.)

The solution for the initial value problem for a specific extension ratio and initial disturbance is shown in Fig. 5. This shows that the a_z wave travels at the basic-state axial velocity W which increases exponentially downstream. Integrating this function shows that the disturbance near the orifice is immediately "felt" at the winder. If the Reynolds number had been nonzero, there would be a finite time required for the disturbance to travel to the winder.

When the winder boundary condition is that of constant force, the disturbances travel only downstream. When the boundary condition is other than that of constant force, the winder partially "reflects" the disturbance back upstream by changing the force in the entire fiber. Depending on the degree of reflection, the disturbance can grow or attenuate.

This interpretation of the mechanism can be used to explain the trends of gravity, surface tension, and inertia found in Fig. 2. Gravity decreases the role of the winder in accelerating the jet, so variations in the force there are not as severe. Hence, gravity stabilizes the fiber. Surface tension has the opposite effect. Increasing inertia is stabilizing because the winder force variations are damped by the inertia of the fiber near the winder. In addition, some unpublished results [15] show that the jet becomes more (less) stable when positive (negative) air drag is added to the fiber model.

Conclusions

We find that draw resonance can be interpreted as a wave phenomenon where the winder can cause wave reflection unless it applies a constant force to the fiber. This realization allows the prediction of trends in fiber-flow instabilities when new physical effects are included in the analysis.

Acknowledgment

The authors acknowledge the support of the Owens/Corning Fiberglass Corporation in funding this research.

References

1 Kase, S., and Matsuo, T., "Studies on Melt Spinning: II. Steady State and Transient Solutions of Fundamental Equations Compared With Experimental Results," *J. Appl. Polymer Sci.*, Vol. 11, 1967, pp. 251–287.

2 Pearson, J. R. A., and Matovich, M. A., "On Spinning a Molten Threadline: Stability," *Ind. Eng. Chem. Fund.*, Vol. 8, 1969, pp. 605–609.

3 Schultz, W. W., and Davis, S. H., "One-Dimensional Liquid Fibers," *J. Rheol.*, Vol. 26, 1982, pp. 331–345.

4 Chang, J. C., Denn, M. M., and Geyling, F. T., "Effects of Inertia, Surface Tension and Gravity on the Stability of Isothermal Drawing of Newtonian Fluids," *Ind. Eng. Chem. Fund.*, Vol. 20, 1981, pp. 147–149.

5 Shah, Y. T., and Pearson, J. R. A., "On the Stability of Nonisothermal Fiber Spinning: General Case," *Ind. Eng. Chem. Fund.*, Vol. 11, 1972, pp. 150–153.

6 Donnelly, G. J., and Weinberger, C. B., "Stability of Isothermal Fiber Spinning of a Newtonian Fluid," *Ind. Eng. Chem. Fund.*, Vol. 14, 1975, pp. 334–337.

7 D'Andrea, R. G., and Weinberger, C. B., "Effects of Surface Tension and Gravity Forces in Determining the Stability of Isothermal Fiber Spinning," *AIChE J.*, Vol. 22, 1976, pp. 923–925.

8 Chang, J. C., and Denn, M. M., "An Experimental Study of Isothermal Spinning of a Newtonian and a Viscoelastic Liquid," *J. Non-Newtonian Fluid Mech.*, Vol. 5, 1979, pp. 369–385.

9 Fisher, R. J., Denn, M. M., and Tanner, R. I., "Initial Profile Development in Melt Spinning," *Ind. Eng. Chem. Fund.*, Vol. 19, 1980, pp. 195–197.

10 Gelder, G., "The Stability of Fiber Drawing Processes," *Ind. Eng. Chem. Fund.*, Vol. 10, 1971, pp. 534–535.

11 Kase, S., and Denn, M. M., "Dynamics of the Melt Spinning Process," *Joint Automatic Control Conference*, Vol. 2, 1978, pp 71–84.

12 White, J. L., and Ide, Y., "Instabilities and Failure in Elongational Flow and Melt Spinning of Fibers," *J. App. Polymer Sci.*, Vol. 22, 1978, pp. 3057–3074.

13 Denn, M. M., "On an Analysis of Draw Resonance by Hyun," *AIChE J.*, Vol. 26, 1980, pp. 292–294.

14 Hyun, J. C., "Theory of Draw Resonance," *AIChE J.*, Vol. 24, 1978, pp. 418–426.

15 Lee, Y., Private Communication, 1983.